ISEF 2011 – XV International Symposium on Electromagnetic Fields
in Mechatronics, Electrical and Electronic Engineering

Funchal, Madeira, September 1-3, 2011

SUBPROBLEM METHOD WITH DUAL FINITE ELEMENT FORMULATIONS FOR ACCURATE THIN SHELL MODELS

Vuong Q. Dang[1], Patrick Dular[1,2], Ruth V. Sabariego[1], Mauricio V. Ferreira da Luz[3], Patrick Kuo-Peng[3], Laurent Krähenbühl[4] and Christophe Geuzaine[1]

[1]University of Liège, Dept. of Electrical Engineering and Computer Science, ACE, B-4000 Liège, Belgium
[2]Fonds de la Recherche Scientifique - F.R.S.-.FNRS, B-1000 Brussels, Belgium
[3]GRUCAD/EEL/CTC/UFSC, P.O. Box 476, 88040-970, Florianopólis, SC, Brazil
[4]University of Lyon, Ampère (CNRS UMR5005), École Centrale de Lyon, F-69134 Écully Cedex, France
ID-56400

Abstract **–** ***A subproblem method with dual finite element magnetostatic and magnetodynamic formulations is developed to correct the inaccuracies near edges and corners coming from thin shell models, that replace thin volume regions by surfaces. The surface-to-volume correction problem is defined as one of the multiple subproblems applied to a complete problem, considering successive additions of inductors and magnetic or conducting regions, some of these being thin regions. Each subproblem is independently solved on its own domain and mesh, which facilitates meshing and solving while controlling the importance and usefulness of each correction. Parameterized analyses of thin regions are efficiently performed.***

Introduction

The finite element (FE) subproblem method (SPM) provides advantages in repetitive analyses and helps improving the solution accuracy [1-2]. Each SP considers the solution of previous SPs through surface sources (SSs) and volume sources (VSs) instead of starting a new complete FE solution for any variation of geometrical or physical data. Each SP is defined on its particular geometry and mesh.

The thin shell (TS) FE representation of thin regions in magnetic problems is herein placed at the hearth of the SPM, to define both parameterized and correction schemes. The TS model is used to avoid meshing the thin regions, and consequently lighten the mesh of their surrounds [3-4]. For that, the volume thin regions are reduced to surfaces with interface conditions (ICs) linked to 1-D analytical distributions (throughout the shell thickness) that however generally neglect end and curvature effects. The SPM with dual finite element $\boldsymbol{b}$- and $\boldsymbol{h}$-formulations are herein applied to correct the inaccuracies of the field distribution and losses proper to the TS FE representation of thin regions, mainly in the vicinity of their edges and corners. Prior to such corrections, the SPM naturally allows parameterized analyses of the thin region characteristics: permeability, conductivity and thickness.

A problem (SP q) with stranded inductors alone is first solved on a simplified mesh without any thin regions. Its solution gives SSs for a TS problem (SP p) via ICs. The solution of SP p is then corrected by a correction problem (SP k) through SSs and VSs, that suppress the TS representation and simultaneously add the actual volume, in order to take the field distribution near edges and corners into account, which are neglected by the TS approximation.

The developments are performed for both magnetic vector potential and magnetic field FE magnetostatic and magnetodynamic formulations, with attention to the proper discretization of the constraints involved in each SP. The method is illustrated and validated on practical test problems.

Magnetic Subproblems of Various Natures

Series of Coupled Subproblems

A complete problem is split into a series of SPs that define a sequence of changes, with the complete solution replaced the sum of the SP solutions. Each SP is defined in its particular domain. It is governed by magnetostatic or magnetodynamic equations and constrained with VSs and SSs [1-2], of which some components originate from previous problems. SSs express changes of ICs through surfaces from SP q to SP p while VSs express changes, from SP p to SP k, of permeability and conductivity of volume regions. Mesh-to-mesh projections are required to express these sources in each new SP [1-2].

The surface-to-volume correction SP consists in suppressing the TS model and simultaneously replacing it by a FE volume model in a domain reduced to the thin region and its surrounds. This is defined via SSs that are the opposite of the so-known TS ICs [1], and simultaneously via VSs expressing the

This work was supported by the Belgian Science Policy (IAP P6/21).

so-considered volume of the thin region that replaces the air region. The SSs have complementary strong and weak natures depending on the $\boldsymbol{b}$- or $\boldsymbol{h}$-formulation used, that necessitate adequate discrete tools to be accurately defined [2]. From a SP p solution with given permeability, conductivity and thickness, a next SP k can consider changes of these parameters directly via SSs that suppress the previous model simultaneously with new TS ICs. All these changes generally lead to local modifications of the solution, which thus allows to reduce the calculation domain and its mesh in the surrounds of the thin regions.

Canonical magnetodynamic or static problem with VSs and SSs

A canonical magnetodynamic or static problem i, to be solved at step i of the SPM, is defined in a domain Ω_i, with boundary $\partial\Omega_i = \Gamma_i = \Gamma_{h,i} \cup \Gamma_{b,i}$. The eddy current conducting part of Ω_i is denoted $\Omega_{c,i}$ and the non-conducting region $\Omega_{c,i}^C$, with $\Omega_i = \Omega_{c,i} \cup \Omega_{c,i}^C$. Stranded inductors belong to $\Omega_{c,i}^C$, whereas massive inductors belong to $\Omega_{c,i}$. The equations, material relations and boundary conditions (BCs) of the SPs i = q, p and k are:

$$\text{curl}\, \boldsymbol{h}_i = \boldsymbol{j}_i \,,\ \text{div}\, \boldsymbol{b}_i = 0 \,,\ \text{curl}\, \boldsymbol{e}_i = -\partial_t \boldsymbol{b}_i \,, \tag{1a-b-c}$$

$$\boldsymbol{h}_i = \mu_i^{-1} \boldsymbol{b}_i + \boldsymbol{h}_{s,i} \,,\ \boldsymbol{b}_i = \mu_i \boldsymbol{h}_i + \boldsymbol{b}_{s,i} \,, \tag{2a-b}$$

$$\boldsymbol{j}_i = \sigma_p \boldsymbol{e}_i + \boldsymbol{j}_{s,i} \,,\ \boldsymbol{e}_i = \sigma_i^{-1} \boldsymbol{j}_i + \boldsymbol{e}_{s,i} \,, \tag{3a-b}$$

$$\boldsymbol{n} \times \boldsymbol{h}_i|_{\Gamma_{h,i}} = \boldsymbol{j}_{su,i} \,,\ \boldsymbol{n} \cdot \boldsymbol{b}_i|_{\Gamma_{b,i}} = \boldsymbol{b}_{su,i} \,,\ \boldsymbol{n} \times \boldsymbol{e}_i|_{\Gamma_{e,i} \subset \Gamma_{b,i}} = \boldsymbol{k}_{su,i} \,, \tag{4a-b-c}$$

where $\boldsymbol{h}_i$ is the magnetic field, $\boldsymbol{b}_i$ is the magnetic flux density, $\boldsymbol{e}_i$ is the electric field, $\boldsymbol{j}_{s,i}$ is the electric current density, μ_i is the magnetic permeability, σ_i is the electric conductivity and $\boldsymbol{n}$ is the unit normal exterior to Ω_i. In what follows the notation $[\cdot]_{\gamma_i} = |_{\gamma_i^+} - |_{\gamma_i^-}$ expresses the discontinuity of a quantity through an interface γ_i (with sides γ_i^+ and γ_i^-) in Ω_i, defining ICs. The fields $\boldsymbol{h}_{s,i}$, $\boldsymbol{b}_{s,i}$, $\boldsymbol{j}_{s,i}$ and $\boldsymbol{e}_{s,i}$ in (2a)-(2b) and (3a)-(3b) respectively are VSs which can be used for expressing changes of permeability or conductivity in each SP.

The fields $\boldsymbol{j}_{su,i}, \boldsymbol{b}_{su,i}$ and $\boldsymbol{k}_{su,i}$ in (4a-b-c) are SSs and generally equal zero with classical homogeneous BCs. Their discontinuities via ICs are also equal to zero, for common continuous field traces $\boldsymbol{n} \times \boldsymbol{h}_i, \boldsymbol{n} \times \boldsymbol{e}_i$ and $\boldsymbol{n} \cdot \boldsymbol{b}_i$. If nonzero, they define possible SSs that account for particular phenomena occuring in the idealized thin region between γ_i^+ and γ_i^- [5], [6]. This is the case when some field traces in SP p are forced to be discontinuous, whereas their continuity must be recovered via a SP k. The SSs in SP q and SP k are to be fixed as the opposite of the trace solution of SP p.

From SP q to SP p - inductor alone to TS model

The constraint for SPs q, p and k are respectively expressed via SSs and VSs. SSs are defined via the BCs and ICs of impedance-type boundary conditions (IBC) combined with contributions from SP q. The TS model [4] for both $\boldsymbol{b}_i$- and $\boldsymbol{h}_i$-formulations requires the unknown discontinuities of $\boldsymbol{a}_{d,t,i}$ and $\boldsymbol{h}_{d,t,i}$ of the tangential components $\boldsymbol{a}_{t,i} = (\boldsymbol{n} \times \boldsymbol{a}_i) \times \boldsymbol{n}$ and $\boldsymbol{h}_{t,i} = (\boldsymbol{n} \times \boldsymbol{h}_i) \times \boldsymbol{n}$ of $\boldsymbol{a}_i$ and $\boldsymbol{h}_i$ through TS, i.e.

$$[\boldsymbol{a}_{t,i}]_{\Gamma_{t,i}} = \boldsymbol{a}_{d,t,i} \ \textit{or}\ [\boldsymbol{n} \times \boldsymbol{a}_{t,i}]_{\Gamma_{t,i}} = \boldsymbol{n} \times \boldsymbol{a}_{t,i} \,, \tag{5}$$

$$[\boldsymbol{h}_{t,i}]_{\Gamma_{ts,i}} = \boldsymbol{h}_{d,t,i} \ \textit{or}\ [\boldsymbol{n} \times \boldsymbol{h}_{t,i}]_{\Gamma_{t,i}} = \boldsymbol{n} \times \boldsymbol{h}_{t,i} \,, \tag{6}$$

where $\boldsymbol{a}_{d,i}$ and $\boldsymbol{h}_{d,i}$ are respectively the discontinuous components of the fields $\boldsymbol{a}_i$ and $\boldsymbol{h}_i$ and defined as equal to zero along the border of the TS, which neglects the magnetic flux entering there. In order to express this discontinuity, based on [4], one has

$$\boldsymbol{a}_i|_{\gamma_{t,i}^+} = \boldsymbol{a}_{c,i} + \boldsymbol{a}_{d,i} \,,\ \boldsymbol{a}_i|_{\gamma_{t,i}^-} = \boldsymbol{a}_{c,i} \,, \tag{7}$$

$$\boldsymbol{h}_i|_{\gamma_{t,i}^+} = \boldsymbol{h}_{c,i} + \boldsymbol{h}_{d,i} \,,\ \boldsymbol{h}_i|_{\gamma_{t,i}^-} = \boldsymbol{h}_{c,i} \,, \tag{8}$$

with $\boldsymbol{a}_{c,i}$ and $\boldsymbol{h}_{c,i}$ are the continuous components and are also applied on $\gamma_{t,i}$ for the tangential components ($\boldsymbol{a}_{t,i}$, $\boldsymbol{a}_{c,t,i}$); ($\boldsymbol{h}_{t,i}$, $\boldsymbol{h}_{c,t,i}$) and ($\boldsymbol{a}_{d,t,i}$, $\boldsymbol{h}_{d,t,i}$).

Let us analyse the contraints between SP q and SP p in both $\boldsymbol{b}$- and $\boldsymbol{h}$-formulations as follows:

Constraint between SP q and SP p for $\boldsymbol{b}$- formulation

Although there is no thin region in SP q, in order to have a relative constraint between SP q and SP p via the corresponding ICs with $\gamma_t = \gamma_t^{\pm} = \gamma_q^{\pm} = \gamma_p^{\pm}$ and $\boldsymbol{n}_t = -\boldsymbol{n}$ for the TS, one has to imagine that a thin region appears in SP q. One gets for SP q and SP p [4],

$$[\boldsymbol{n} \times \boldsymbol{h}_q]_{\gamma_q} = \boldsymbol{n} \times \boldsymbol{h}_q|_{\gamma_q^+} - \boldsymbol{n} \times \boldsymbol{h}_q|_{\gamma_q^-} = 0, \tag{9}$$

$$[\boldsymbol{n} \times \boldsymbol{h}]_{\gamma_p} = [\boldsymbol{n} \times \boldsymbol{h}_q]_{\gamma_p} + [\boldsymbol{n} \times \boldsymbol{h}_p]_{\gamma_p} = -\sigma\beta\,\partial_t(2\boldsymbol{a}_c + \boldsymbol{a}_d), \tag{10}$$

$$\boldsymbol{n} \times \boldsymbol{h}_p|_{\gamma_p^+} = \frac{1}{2}\big[\sigma\beta\,\partial_t(2\boldsymbol{a}_c + \boldsymbol{a}_d) + \frac{1}{\mu\beta}\,\boldsymbol{a}_d\big] - \boldsymbol{n} \times \boldsymbol{h}_q|_{\gamma_p^+}, \tag{11}$$

$$\beta = \gamma_i^{-1}\tanh(\frac{d_i\gamma_i}{2}), \gamma_i = \frac{1+j}{\delta_i}, \delta_i = \sqrt{\frac{2}{\omega\sigma_i\mu_i}}, \tag{12}$$

where d_i is the local TS thickness, δ_i is the skin depth in the TS, $\omega = 2\pi f$ with f is the frequency, j is the imaginary unit and $\partial_t \equiv j\omega$. For $\delta_i \gg d_i$, one has $\beta \approx d_i/2$. In statics, (10) is equal to zero. The discontinuity $[\boldsymbol{n} \times \boldsymbol{h}_q]_{\gamma_p}$ in (10) does not need any correction because solution SP q presents no such discontinuitiy, i.e. $[\boldsymbol{n} \times \boldsymbol{h}_q]_{\gamma_q} = [\boldsymbol{n} \times \boldsymbol{h}_q]_{\gamma_p} = 0$.

Constraint between SP q and SP p for $\boldsymbol{h}$- formulation

One has for SP q and SP p [4],

$$[\boldsymbol{n} \times \boldsymbol{e}_q]_{\gamma_q} = \boldsymbol{n} \times \boldsymbol{e}_q|_{\gamma_q^+} - \boldsymbol{n} \times \boldsymbol{e}_q|_{\gamma_q^-} = 0, \tag{13}$$

$$[\boldsymbol{n} \times \boldsymbol{e}]_{\gamma_p} = [\boldsymbol{n} \times \boldsymbol{e}_q]_{\gamma_p} + [\boldsymbol{n} \times \boldsymbol{e}_p]_{\gamma_p} = -\sigma\beta\,\partial_t(2\boldsymbol{h}_c + \boldsymbol{h}_d), \tag{14}$$

$$\boldsymbol{n} \times \boldsymbol{e}_p|_{\gamma_p^+} = \frac{1}{2}\big[\sigma\beta\,\partial_t(2\boldsymbol{h}_c + \boldsymbol{h}_d) + \frac{1}{\mu\beta}\,\boldsymbol{h}_d\big] - \boldsymbol{n} \times \boldsymbol{e}_q|_{\gamma_p^+}. \tag{15}$$

Analogously, for $\boldsymbol{b}$- formulation in statics, (14) is zero. The discontinuity $[\boldsymbol{n} \times \boldsymbol{e}_q]_{\gamma_p}$ in (14) also does not need any correction because solution SP q verifies $[\boldsymbol{n} \times \boldsymbol{e}_q]_{\gamma_q} = [\boldsymbol{n} \times \boldsymbol{e}_q]_{\gamma_p} = 0$.

From SP p to SP k - TS to volume model

Once obtained, the TS solution of SP p is then corrected by SP k that overcomes the TS assumptions [4]. SPM offers the tools to implement such as refinement, thanks to simultaneous SSs and VSs. It has to suppress the TS representation via SSs opposed to TS ICs, in parallel to VSs in added the volumic shell via VSs that account for volumic change of μ_k and σ_k in SP k that characterized the ambient region (with $\mu_p = \mu_0$, $\mu_k = \mu_{volume}$, $\sigma_p = 0$ and $\sigma_k = \sigma_{volume}$). This correction will be shown to be limited to the neighborhood of the shell, which permits to benefit from a reduction of the extension of the associated mesh [1]. Indeed, for changes in a region, from μ_p and σ_p in SP p to μ_k and σ_k in SP k, one has the associated VSs,

$$\boldsymbol{h}_{s,k} = (\mu_k^{-1} - \mu_p^{-1})\boldsymbol{b}_p\,,\ \boldsymbol{b}_{s,k} = (\mu_k - \mu_p)\boldsymbol{h}_p\,, \tag{16a-b}$$

$$\boldsymbol{j}_{s,k} = (\sigma_k - \sigma_p)\boldsymbol{e}_p\,,\ \boldsymbol{e}_{s,k} = (\sigma_k^{-1} - \sigma_p^{-1})\boldsymbol{j}_p\,. \tag{17a-b}$$

Finite element weak formulations

$\boldsymbol{b}$- formulation - Magnetic Vector Potential Formulation

The weak $\boldsymbol{b}_i$-formulation is obtained from the weak form of the Ampere's law (1a), i.e. [5]-[6]. For SPs q and p, they have

$$\begin{aligned}(\mu_q^{-1}\mathrm{curl}\,\boldsymbol{a}_q, \mathrm{curl}\,\boldsymbol{a}'_q)_{\Omega_q} + (\sigma_q\partial_t\boldsymbol{a}_q, \boldsymbol{a}'_q)_{\Omega_q} + (\sigma_q\mathrm{grad}\,v_q, \boldsymbol{a}'_q)_{\Omega_q} + \langle\boldsymbol{n} \times \boldsymbol{h}_q, \boldsymbol{a}'_q\rangle_{\Gamma_{h,q}} + \langle\boldsymbol{n} \times \boldsymbol{h}_q, \boldsymbol{a}'_q\rangle_{\Gamma_{b,q}} \\ + \langle[\boldsymbol{n} \times \boldsymbol{h}_q]_{\gamma_q}, \boldsymbol{a}'_q\rangle_{\gamma_q} = (\boldsymbol{j}_{s,q}, \boldsymbol{a}'_q)_{\Omega_q}\,,\ \forall\boldsymbol{a}'_q \in F_q^1(\Omega_q)\,,\end{aligned} \tag{18}$$

$$(\mu_p^{-1}\text{curl}\,\boldsymbol{a}_p,\text{curl}\,\boldsymbol{a}'_p)_{\Omega_p}+(\sigma_p\partial_t\boldsymbol{a}_p,\boldsymbol{a}'_p)_{\Omega_p}+(\sigma_p\text{grad}\,v_p,\boldsymbol{a}'_p)_{\Omega_p}+\langle\boldsymbol{n}\times\boldsymbol{h}_p,\boldsymbol{a}'_p\rangle_{\Gamma_{h,p}}+\langle\boldsymbol{n}\times\boldsymbol{h}_p,\boldsymbol{a}'_p\rangle_{\Gamma_{b,p}}$$
$$+\langle[\boldsymbol{n}\times\boldsymbol{h}_p]_{\gamma_p},\boldsymbol{a}'_c\rangle_{\gamma_p}\,,\forall\boldsymbol{a}'_p\in F_p^1(\Omega_p)\,, \tag{19}$$

where $F_i^1(\Omega_i)$ in (18) and (19) is a gauged curl-conform function space defined on Ω_i, gauged in $\Omega_{c,i}^C$, and containing the basis functions for $\boldsymbol{a}_i$ as well as for the test function $\boldsymbol{a}'_i$ (at the discrete level, this space is defined by edge FEs; the gauge is based on the tree-cotree technique); $(\cdot\,,\cdot)_{\Omega_i}$ and $<\,\cdot\,,\cdot\,>_{\Gamma_i}$ respectively denote a volume intergal in Ω_i and a surface intergal on Γ_i of the product of their vector field arguments. The surface integral term on $\Gamma_{h,i}$ accounts for natural BCs of type (3a), usually zero. The unknown term on the surface $\Gamma_{b,i}$ with essential BCs on $\boldsymbol{n}.\boldsymbol{b}_i$ is often omitted because it does not locally contribute to (18). It will be shown to be the key for the post-processing a solution, a part of which $\boldsymbol{n}\times\boldsymbol{h}_i|_{\Gamma_{b,i}}$ having to act further as a SS [5], [6]. The term $\langle[\boldsymbol{n}\times\boldsymbol{h}_p]_{\gamma_p},\boldsymbol{a}'_p\rangle_{\gamma_p}$ in (19) is rewritten as:

$$\langle[\boldsymbol{n}\times\boldsymbol{h}_p]_{\gamma_p},\boldsymbol{a}'_p\rangle_{\gamma_p}=\langle[\boldsymbol{n}\times\boldsymbol{h}_p]_{\gamma_p},\boldsymbol{a}'_c+\boldsymbol{a}'_d\rangle_{\gamma_p}=\langle[\boldsymbol{n}\times\boldsymbol{h}_p]_{\gamma_p},\boldsymbol{a}'_c\rangle_{\gamma_p}+\langle[\boldsymbol{n}\times\boldsymbol{h}_p]_{\gamma_p},\boldsymbol{a}'_d\rangle_{\gamma_p}, \tag{20}$$

where $\boldsymbol{a}'_d$ and $\boldsymbol{a}'_c$ are the test functions; $\boldsymbol{a}'_d$ is defined as equal to zero on the negative side $\Gamma_{t,p}^-=\gamma_{t,p}^-$ of the TS [4]. In order to explicitly present the field discontinuities, the equation (20) can be also rewritten as

$$\langle[\boldsymbol{n}\times\boldsymbol{h}_p]_{\gamma_p},\boldsymbol{a}'_p\rangle_{\gamma_p}=\langle[\boldsymbol{n}\times\boldsymbol{h}_p]_{\gamma_p},\boldsymbol{a}'_c\rangle_{\gamma_p}+\langle\boldsymbol{n}\times\boldsymbol{h}_p|_{\gamma_p^+},\boldsymbol{a}'_d\rangle_{\gamma_{p^+}}. \tag{21}$$

The $\boldsymbol{h}_i$ trace discontinuity $\langle[\boldsymbol{n}\times\boldsymbol{h}_p]_{\gamma_p},\boldsymbol{a}'_c\rangle_{\gamma_p}$ in (21) is given by (10), i.e.

$$\langle[\boldsymbol{n}\times\boldsymbol{h}]_{\gamma_p},\boldsymbol{a}'_c\rangle_{\gamma_p}=\langle[\boldsymbol{n}\times\boldsymbol{h}_p]_{\gamma_p},\boldsymbol{a}'_c\rangle_{\gamma_p}=\langle\sigma\beta\,\partial_t(2\boldsymbol{a}_c+\boldsymbol{a}_d),\boldsymbol{a}'_c\rangle_{\gamma_p}. \tag{22}$$

The term $\langle\boldsymbol{n}\times\boldsymbol{h}_p|_{\gamma_p^+},\boldsymbol{a}'_d\rangle_{\gamma_{p^+}}$ in (21) related to the positive side of the TS is given by (11), suppressing $\boldsymbol{n}\times\boldsymbol{h}_q|_{\gamma_p^+}$ of SP q and adding the actual TS BC. For that, the resulting surface integral term $\langle\boldsymbol{n}\times\boldsymbol{h}_q|_{\gamma_p^+},\boldsymbol{a}'_d\rangle_{\gamma_{p^+}}$ is a SS that can be correctly expressed via the weak formulation of SP q in (18), ie.

$$-\langle\boldsymbol{n}\times\boldsymbol{h}_q|_{\gamma_p^+},\boldsymbol{a}'_d\rangle_{\gamma_p^+}=(\mu_q^{-1}\text{curl}\,\boldsymbol{a}_q,\text{curl}\,\boldsymbol{a}'_d)_{\Omega_{q=p}}+(\sigma_q\partial_t\boldsymbol{a}_q,\boldsymbol{a}'_d)_{\Omega_{q=p}}+(\sigma_q\text{grad}\,v_q,\boldsymbol{a}'_d)_{\Omega_{q=p}}, \tag{23}$$

where v_q is an electric scalar potential defined in added conducting regions in [6]. The contributions in the volume integrals in (23) are limited to a single layer of FEs on the posittive side of $\Omega_p^+=\Omega_q^+$ touching $\gamma_p^+=\gamma_q^+$, because it involves only the traces $\boldsymbol{n}\times\boldsymbol{a}'_d|_{\gamma_p^+}$. One should note that σ_q = 0 for SP q (inductors alone). At the discrete level, the source $\boldsymbol{a}_q$, initially in mesh of SP q, has to be projected in mesh of SP p [1], [8]. The obtained solution of TS SP p in (19) is then corrected by SP k via the VSs by (16a) and (17a). Moreover, fields have to be also transferred from the mesh of SP p to the mesh of SP k. The weak form for SP k is then

$$(\mu_k^{-1}\text{curl}\,\boldsymbol{a}_k,\text{curl}\,\boldsymbol{a}'_k)_{\Omega_k}+(\sigma_k\,\partial_t\boldsymbol{a}_k,\boldsymbol{a}'_k)_{\Omega_{ck}}+(\sigma_k\,\text{grad}\,v_k,\boldsymbol{a}'_k)_{\Omega_{ck}}+(\boldsymbol{h}_{s,k},\text{curl}\,\boldsymbol{a}'_k)_{\Omega_k}$$
$$+(\boldsymbol{j}_{s,k},\boldsymbol{a}'_k)_{\Omega_{c,k}}+\langle\boldsymbol{n}\times\boldsymbol{h}_k,\boldsymbol{a}'_k\rangle_{\Gamma_{h,k}}+\langle\boldsymbol{n}\times\boldsymbol{h}_k,\boldsymbol{a}'_k\rangle_{\Gamma_{b,k}}=0,\forall\boldsymbol{a}'_k\in F_k^1(\Omega_k)\,. \tag{24}$$

$\boldsymbol{h}$- formulation - Magnetic Field Formulation

The weak $\boldsymbol{h}_i$-formulation is written as the weak form of the Faraday's law (1c) [5], [6]. The field $\boldsymbol{h}_i$ is decomposed into two parts, $\boldsymbol{h}_i=\boldsymbol{h}_{s,i}+\boldsymbol{h}_{r,i}$, where $\boldsymbol{h}_{s,i}$ is the source field defined through $\text{curl}\,\boldsymbol{h}_{s,i}=\boldsymbol{j}_{s,i}$, and $\boldsymbol{h}_{r,i}$ is the reaction magnetic field. The weak forms for SPs q and p are

$$\partial_t(\mu_q^{-1}\boldsymbol{h}_q,\boldsymbol{h}'_q)_{\Omega_q}+\partial_t(\mu_q^{-1}\boldsymbol{h}_{s,q},\boldsymbol{h}'_q)_{\Omega_q}+\langle\boldsymbol{n}\times\boldsymbol{e}_q,\boldsymbol{h}'_q\rangle_{\Gamma_{e,q}}+\langle[\boldsymbol{n}\times\boldsymbol{e}_q]_{\gamma_q},\boldsymbol{h}'_q\rangle_{\gamma_q}=0\,,$$
$$\forall\boldsymbol{h}'_q\in F_q^1(\Omega_q)\,, \tag{25}$$
$$\partial_t(\mu_p^{-1}\boldsymbol{h}_p,\boldsymbol{h}'_p)_{\Omega_p}+(\sigma_p^{-1}\text{curl}\,\boldsymbol{h}_p,\text{curl}\,\boldsymbol{h}'_p)_{\Omega_p}+\langle\boldsymbol{n}\times\boldsymbol{e}_p,\boldsymbol{h}'_p\rangle_{\Gamma_{e,p}}+\langle[\boldsymbol{n}\times\boldsymbol{e}_p]_{\gamma_p},\boldsymbol{h}'_p\rangle_{\gamma_p}=0\,,$$
$$\forall\boldsymbol{h}'_p\in F_p^1(\Omega_p)\,, \tag{26}$$

where $F_i^1(\Omega_i)$ is the curl-conform function space defined on Ω_i and containing the basis functions for $\boldsymbol{h}_i$ as well as for the test function $\boldsymbol{h}'_i$. The surface integral terms on $\Gamma_{e,i}$ account for natural BCs of type (4c), usually zero. The term $\langle[\boldsymbol{n}\times\boldsymbol{e}_p]_{\gamma_p},\boldsymbol{h}'_p\rangle_{\gamma_p}$ in (26) reads as

$$\langle[\boldsymbol{n}\times\boldsymbol{e}_p]_{\gamma_p},\boldsymbol{h}'_p\rangle_{\gamma_p}=\langle[\boldsymbol{n}\times\boldsymbol{e}_p]_{\gamma_p},\boldsymbol{h}'_c+\boldsymbol{h}'_d\rangle_{\gamma_p}=\langle[\boldsymbol{n}\times\boldsymbol{e}_p]_{\gamma_p},\boldsymbol{h}'_c\rangle_{\gamma_p}+\langle[\boldsymbol{n}\times\boldsymbol{e}_p]_{\gamma_p},\boldsymbol{h}'_d\rangle_{\gamma_p}, \tag{27}$$

where $\boldsymbol{h}'_d$ and $\boldsymbol{h}'_c$ are the test functions; $\boldsymbol{h}'_d$ is also zero on the negative side of TS γ_p^- [4]. The field discontinuity term in (27) becomes

$$\langle[\boldsymbol{n}\times\boldsymbol{e}_p]_{\gamma_p},\boldsymbol{h}'_p\rangle_{\gamma_p}=\langle[\boldsymbol{n}\times\boldsymbol{e}_p]_{\gamma_p},\boldsymbol{h}'_c\rangle_{\gamma_p}+\langle\boldsymbol{n}\times\boldsymbol{e}_p|_{\gamma_{p^+}},\boldsymbol{h}'_d\rangle_{\gamma_{p^+}}. \tag{28}$$

The $\boldsymbol{e}_i$ trace discontinuity $\langle[\boldsymbol{n}\times\boldsymbol{e}_p]_{\gamma_p},\boldsymbol{h}'_c\rangle_{\gamma_p}$ in (28) is given by (14), i.e.

$$\langle[\boldsymbol{n}\times\boldsymbol{e}_p]_{\gamma_p},\boldsymbol{h}'_c\rangle_{\gamma_p}=\langle[\boldsymbol{n}\times\boldsymbol{e}]_{\gamma_p},\boldsymbol{h}'_c\rangle_{\gamma_p}=\langle\sigma\beta\,\partial_t(2\boldsymbol{h}_c+\boldsymbol{h}_d),\boldsymbol{h}'_c\rangle_{\gamma_p}. \tag{29}$$

The other term $\langle\boldsymbol{n}\times\boldsymbol{e}_p|_{\gamma_{p^+}},\boldsymbol{h}'_d\rangle_{\gamma_{p^+}}$ in (28) is given by (15), suppressing $\boldsymbol{n}\times\boldsymbol{e}_q|_{\gamma_{p^+}}$ of SP q and in the same time adding the actual TS BC. For that, the term $\langle\boldsymbol{n}\times\boldsymbol{e}_p|_{\gamma_{p^+}},\boldsymbol{h}'_d\rangle_{\gamma_{p^+}}$ is a SS that is naturally expressed via the weak formulation of SP q in (25), i.e.

$$-\langle\boldsymbol{n}\times\boldsymbol{e}_q|_{\gamma_p^+},\boldsymbol{h}'_d\rangle_{\gamma_p^+}=(\mu_q\partial_t\boldsymbol{h}_{s,q},\boldsymbol{h}'_d)_{\Omega_p=\Omega_q}+(\mu_q\partial_t\boldsymbol{h}_q,\boldsymbol{h}'_d)_{\Omega_p=\Omega_q}. \tag{30}$$

The volume integrals in (30) are also limited to a single layer of FEs touching $\gamma_p^+=\gamma_q^+$, because they involve only the traces $\boldsymbol{n}\times\boldsymbol{h}'_d|_{\gamma_p^+}$. At the discrete level, the source $\boldsymbol{h}_q$, initially in mesh of SP q, has to be projected in mesh of SP p [1], [8]. Then the actual volume SP k corrects the inaccurate TS SP p solution via the VSs in (16b) and (17b). The weak form of SP k is

$$\begin{aligned}\partial_t(\mu_k\boldsymbol{h}_k,\boldsymbol{h}'_k)_{\Omega_k}+(\sigma_k^{-1}\mathrm{curl}\,\boldsymbol{h}_k,\mathrm{curl}\,\boldsymbol{h}'_k)_{\Omega_k}+\partial_t(\boldsymbol{b}_{s,k},\boldsymbol{h}'_k)_{\Omega_k}+(\boldsymbol{e}_{s,k},\mathrm{curl}\,\boldsymbol{h}'_k)_{\Omega_k}\\ +\langle\boldsymbol{n}\times\boldsymbol{e}_k,\boldsymbol{h}'_k\rangle_{\Gamma_{e,k}}=0,\forall\boldsymbol{h}'_k\in F_k^1(\Omega_k)\,.\end{aligned} \tag{31}$$

TS Correction-VSs in the Actual Volumic Shell and SSs for Suppressing the TS Representation

Changes of material properties from μ_p and σ_p in SP p to μ_k and σ_k in SP k, that occur in the volumic shell, are taken into account in (24) and (31) via the volume integrals $(\boldsymbol{h}_{s,k},\mathrm{curl}\,\boldsymbol{a}'_k)_{\Omega_k}$, $(\boldsymbol{j}_{s,k},\boldsymbol{a}'_k)_{\Omega_{c,k}}$ and $(\boldsymbol{e}_{s,k},\mathrm{curl}\,\boldsymbol{h}'_k)_{\Omega_k}$, $\partial_t(\boldsymbol{b}_{s,k},\boldsymbol{h}'_k)_{\Omega_k}$. The VS $\boldsymbol{b}_{s,k}$ and $\boldsymbol{h}_{s,k}$ are respectively given by (16a) and (16b), with $\boldsymbol{b}_i=\mathrm{curl}\,\boldsymbol{a}_i$. The VS $\boldsymbol{j}_{s,k}$ is given by (17a), generally reduced to $\boldsymbol{j}_{s,k}=\sigma_k\boldsymbol{e}_p=\sigma_k(-\partial_t\boldsymbol{a}_p-\mathrm{grad}\,v_p)$. Potential v_p can be usually fixed to zezo. The VS $\boldsymbol{e}_{s,k}$ in (17b) is to be obtained from the still undetermined electric field $\boldsymbol{e}_p$, with $\boldsymbol{e}_{s,k}=(\sigma_p/\sigma_k\text{-}1)\boldsymbol{e}_p$. Therefore, the field $\boldsymbol{e}_p$ is unknown in any $\Omega_{c,p}^C$. Thus the determination of $\boldsymbol{e}_p$ requires to solve an electric problem defined by the Faraday and electric conservation equations [6].

Simultaneously to the VSs, SSs have to suppress the TS discontinuities. They can be defined via ICs as

$$[\boldsymbol{n}\times\boldsymbol{h}_k]_{\gamma_{t,k}}=-[\boldsymbol{n}\times\boldsymbol{h}_p]_{\gamma_{t,k}},[\boldsymbol{n}\times\boldsymbol{a}_k]_{\gamma_{t,k}}=-\boldsymbol{n}\times\boldsymbol{a}_p|_{\gamma_{t,k}}, \tag{32a-b}$$

$$[\boldsymbol{n}\times\boldsymbol{e}_k]_{\gamma_{t,k}}=-[\boldsymbol{n}\times\boldsymbol{e}_p]_{\gamma_{t,k}},[\boldsymbol{n}\times\boldsymbol{h}_k]_{\gamma_{t,k}}=-\boldsymbol{n}\times\boldsymbol{h}_p|_{\gamma_{t,k}}, \tag{33a-b}$$

respectively for $\boldsymbol{b}$- and $\boldsymbol{h}$-formulations. ICs (32b) and (33b) strongly fixe $\boldsymbol{a}_{d,t,k}=-\boldsymbol{a}_{d,t,p}$ and $\boldsymbol{h}_{d,t,k}=-\boldsymbol{h}_{d,t,p}$. IC (32a) and (33a) are weakly expressed through the last integrals in (24) and (31), with $\gamma_{t,k}=\gamma_{t,p}$. The involved traces $[\boldsymbol{n}\times\boldsymbol{h}_p]_{\gamma_{t,k}}$ and $[\boldsymbol{n}\times\boldsymbol{e}_p]_{\gamma_{t,k}}$ are naturally expressed via the other volume integrals in (19) and (26), i.e.

$$\langle[\boldsymbol{n}\times\boldsymbol{h}_k]_{\gamma_{t,k}},\boldsymbol{a}'_k\rangle_{\gamma_{t,k}}=-\langle[\boldsymbol{n}\times\boldsymbol{h}_p]_{\gamma_{t,k}},\boldsymbol{a}'_k\rangle_{\gamma_{t,p}}, \tag{34}$$

$$\langle[\boldsymbol{n}\times\boldsymbol{e}_k]_{\gamma_{t,k}},\boldsymbol{h}'_k\rangle_{\gamma_{t,k}}=-\langle[\boldsymbol{n}\times\boldsymbol{h}_p]_{\gamma_{t,k}},\boldsymbol{h}'_k\rangle_{\gamma_{t,p}}. \tag{35}$$

The surface integrals in (34) and (35) are used at step i. At the discrete level, these are limited to the layers of FEs on both sides $\gamma_{t,k}$ of TS, because they involve only the associated traces $\boldsymbol{n}\times\boldsymbol{a}'_k|_{\gamma_{t,k}}$ and $\boldsymbol{n}\times\boldsymbol{h}'_k|_{\gamma_{t,k}}$. For the sources $\boldsymbol{a}_p$ and $\boldsymbol{h}_p$ containing their discontinuities $\boldsymbol{a}_{d,p}$ and $\boldsymbol{h}_{d,p}$, are initially given in mesh of SP p, have to be projected in mesh of SP k [1],[8].

Application Example

The test problem is based on TEAM problem 21 (model B), with two inductors and a thin plate (Fig. 1(a)). An example of magnetodynamic SP scheme is tested in both 2-D and 3-D cases.

The first test of a 2-D model considers three SPs: a first SP q with the inductors alone solved on a simplified mesh without any thin regions (Fig. 2($\boldsymbol{a}_1$), *top left*); a TS FE SP p (Fig. 2($\boldsymbol{a}_2$), *top right*) that does not include the inductors anymore; a correction SP k replacing the TS FEs with the actual volume FEs covering the actual plates with an adequate refined mesh (Fig. 2($\boldsymbol{a}_3$), *bottom middle*). The projection of SP q solution in the TS SP p and of the TS SP p in the SP k are respectively illustrated (Fig. 2($\boldsymbol{a}_{proj}$,SS), *top middle*) and (Fig. 2($\boldsymbol{a}_{proj}$,VS), *bottom left*). The complete solution is finally shown as well (Fig. 2($\boldsymbol{a} = \boldsymbol{a}_1 + \boldsymbol{a}_2 + \boldsymbol{a}_3$), *bottom right*). The errors on the power loss density of TS SP p along the plate are pointed out by the correction SP k (Figs. 3(a), 3(b)) for different parameters. They reach 40% for both $\boldsymbol{b}$- and $\boldsymbol{h}$-formulations ($\delta = 1.977$mm, d = 7.5mm). Significant error decreases with a thinner thickness, being lower than 5% (d = 1.5mm).

The second test of a 2-D model considers two SPs: a SP q with the inductors and a thin plate; a surface-to-volume correction SP k. The relative corrections of the power loss density and the longitudinal magnetic flux along the plate are shown in Fig. 4. They reach several tens of percents in the TS, such as 70% (Fig. 4(a)) and 75% (Fig. 4(b)) near the plate ends, with $\delta = 1.977$mm and d = 7.5mm in both cases. For the smaller thicknesses, the errors are lower than 30% (d = 3mm) (Fig. 4(a)) and 20% (d = 1.5mm) (Fig. 4(a), 4(b)). For the case of non-magnetic material, the error is also up to 42.5% (Fig. 4(b)).

Finally, a 3-D model considers three SPs q, p and k (Figs. 5, 6 and 7). The inccuracies on the eddy current densities of TS SP p are pointed out by the importance of the correction SP k (Figs. 5(a), 5(b)). The error on TS SP p solution along the horizontal half inner (y-direction) reaches 64% in the end regions of the plate (Fig. 5(a)), or 50% along the vertical half edge (z-direction) (Fig. 5(b)), with $\delta = 2.1$mm and d = 7.5mm in both cases. Significant errors on the power loss density reach 85% along the y-direction (Fig. 6(a)), or being 68% along the z-direction (Fig. 6(b)) ($\delta = 2.1$mm, d = 7.5mm) as well. The errors particularly decrease with a smaller thickness (d = 1.5mm), being lower than 20% in both Figs. 5(a), 5(b) and Figs. 6(a), 6(b). For the non-magnetic material, the error is 37.5% (d = 10mm), or lower than 5% (d = 1.5mm) (Fig. 7(b)), with δ = 1.31mm in both cases. The relative correction on the power loss density is also pointed out in Fig. 7(a) with several parameters, up to 85% in the end regions of the plate ($\delta = 1.977$mm, d = 7.5mm). Distributions of eddy current densities on the TS SP p and SP k for d = 7.5mm are shown in Fig. 1(b), 1(c). Some TS inaccuracies are illustrated in Fig. 1(d), 1(e), showing errors near the plate ends, that grow with the plate thickness.

Conclusions

All the steps of the method for TS FE have been presented and validated by coupling subproblems via SPM in both $\boldsymbol{b}$- and $\boldsymbol{h}$- formumations. A general SP scheme with inductors alone, TS regions added, TS parameter changes and corresponding surface-to-volume corrections is applied and validated for both 2-D and 3-D models, allowing to point out its efficiency and accuracy in parameterized analyses. Accurate magnetic flux distributions, eddy current and power loss density are successfully obtained at the edges and corners of the thin regions.

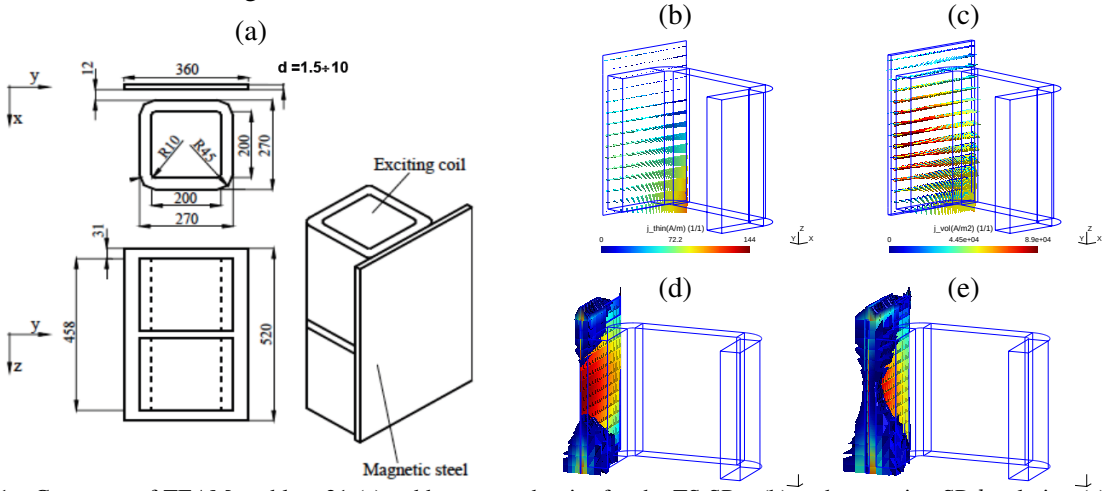

Fig. 1. Geometry of TEAM problem 21 (a); eddy current density for the TS SP p (b) and correction SP k solution (c), with error reaching 78.4% (d =7.5mm); colored map pointing out the regions with a relative correction higher than 1% (in the plates and the vicinity of their ends), with d = 1.5mm (d) and d = 7.5mm (e) ($\mu_{plate} = 200$, $\sigma_{plate} = 6.484$ MS/m, f = 50 Hz).

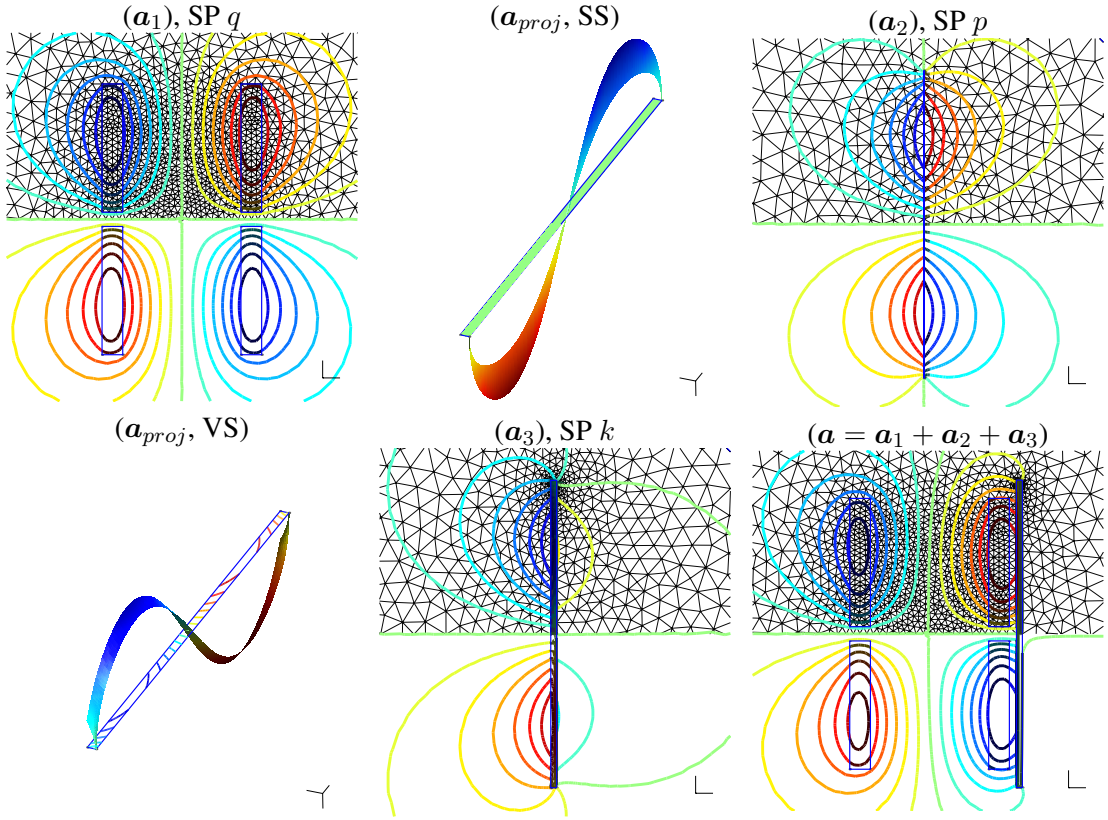

Fig. 2. Flux lines for the magnetodynamic stranded inductor model SP q ($\boldsymbol{a}_1$), TS SP p added ($\boldsymbol{a}_2$), correction solution SP k ($\boldsymbol{a}_3$) and the complete solution (SP q + SP p + SP k = $\boldsymbol{a} = \boldsymbol{a}_1 + \boldsymbol{a}_2 + \boldsymbol{a}_3$) with the different meshes used ($f = 50$ Hz, $\mu_{plate} = 200$, $\sigma_{plate} = 6.484$ MS/m). Projection of SP q solution ($\boldsymbol{a}_{proj}$,SS) in the SP p, and of SP p ($\boldsymbol{a}_{proj}$,VS) in the SP k.

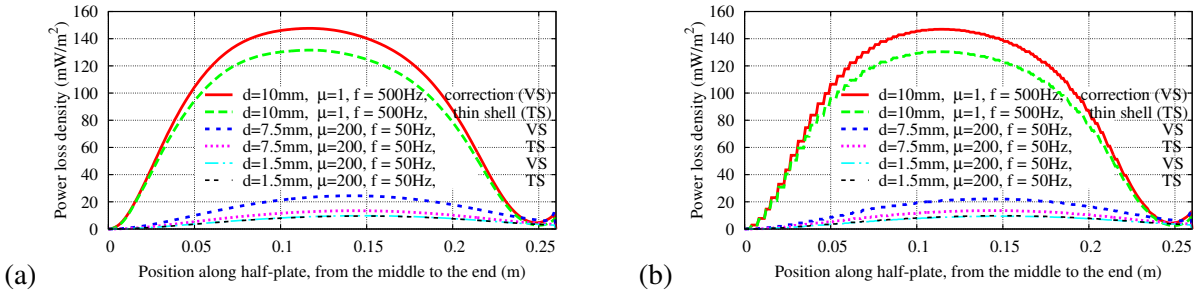

Fig. 3. Power loss density between TS and VS solution along the plate for $\boldsymbol{b}$-formulation (a) and $\boldsymbol{h}$-formulation (b), with effects of d, μ_r and f for 2-D model ($\sigma_{plate} = 6.484$ MS/m).

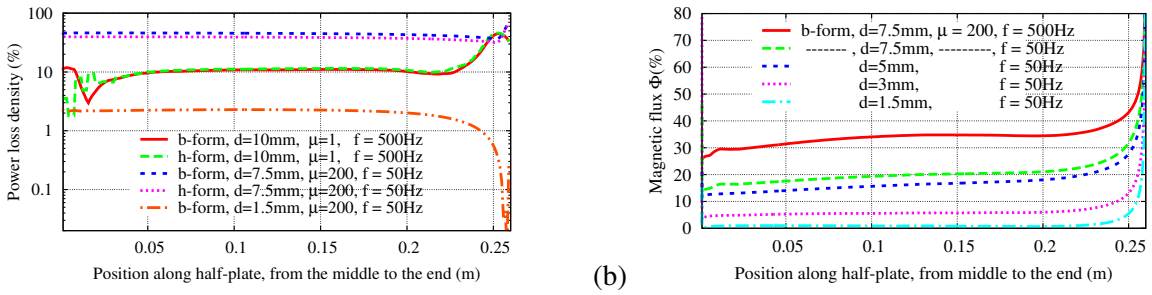

Fig. 4. Relative correction of the power loss density (a) and of the longitudinal magnetic flux (b) along the plate, with effects of d, μ_r, and f for 2-D model ($\sigma_{plate} = 6.484$ MS/m).

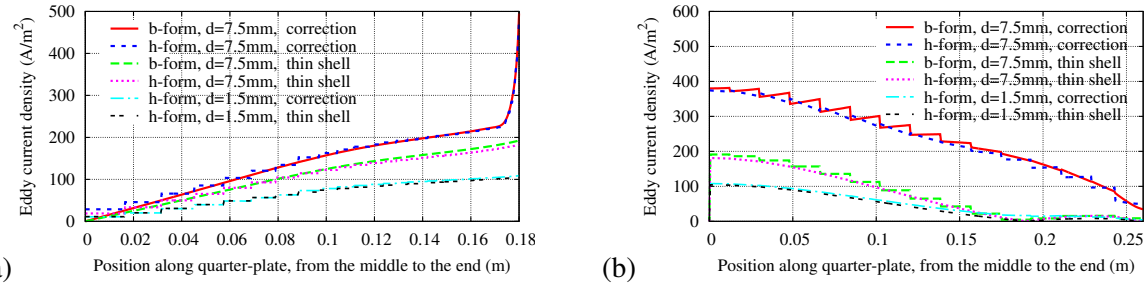

Fig. 5. Eddy current density between TS and VS solution along horizontal half inner width (y-direction) (a) and vertical half edge (z-direction) (b), with effects of d for 3-D model (μ_{plate} = 200, σ_{plate} = 6.484 MS/m, f = 50 Hz).

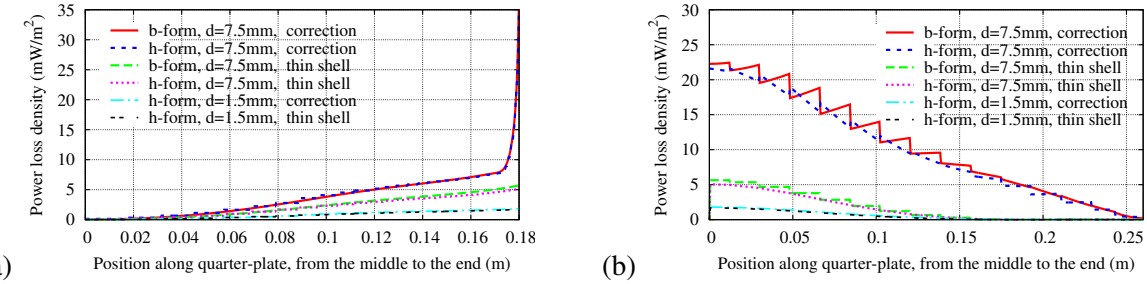

Fig. 6. Power loss density between TS and VS solution along horizontal half inner width (y-direction) (a) and vertical half edge (z-direction) (b), with effects of d for 3-D model (μ_{plate} = 200, σ_{plate} = 6.484 MS/m, f = 50 Hz).

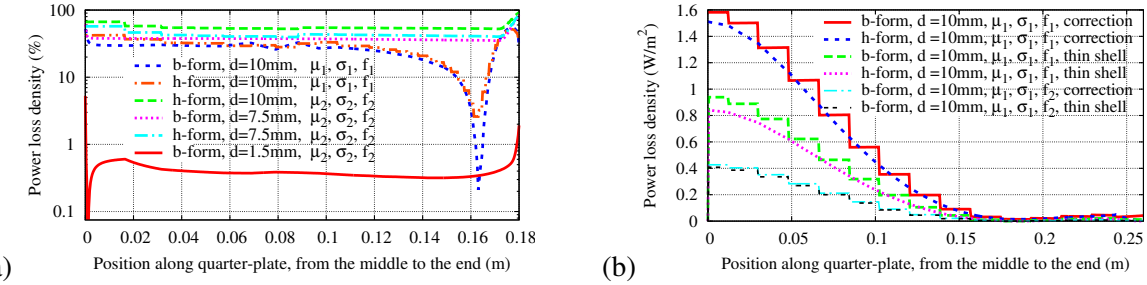

Fig. 7. Relative correction of the power loss density (a) along the plate; power loss density between thin shell and correction solution along vertical half edge (z-direction) (b), with 3-D model (μ_1 = 1, μ_2 = 200, σ_1 = 59 MS/m, σ_2 = 6.484 MS/m, f_1 = 250 Hz, f_2 = 50 Hz).

References

[1] P. Dular, Vuong Q. Dang, R. V. Sabariego, L. Krähenbühl and C. Geuzaine, "Correction of thin shell finite element magnetic models via a subproblem method," IEEE Trans. Magn., vol. 47, no. 5, pp. 158 –1161, 2011.

[2] P. Dular, R. V. Sabariego, C. Geuzaine, M. V. Ferreira da Luz, P. Kuo-Peng and L. Krähenbühl, "Finite Element Magnetic Models via a Coupling of Subproblems of Lower Dimensions," IEEE Trans. Magn., vol. 46, no. 8, pp. 2827–2830, 2010.

[3] L. Krähenbühl and D. Muller, "Thin layers in electrical engineering. Examples of shell models in analyzing eddy- currents by boundary and finite element methods," IEEE Trans. Magn., vol. 29, no. 2, pp. 1450–1455, 1993.

[4] C. Geuzaine, P. Dular, and W. Legros, "Dual formulations for the modeling of thin electromagnetic shells using edge elements," IEEE Trans. Magn., vol. 36, no. 4, pp. 799–802, 2000.

[5] P. Dular, R. V. Sabariego and L. Krähenbühl, "Magnetic Model Refinement via a Perturbation Finite Element Method - From 1-D to 3-D," COMPEL, vol. 28, no. 4, pp. 974-988, 2009.

[6] P. Dular and R. V. Sabariego, "A perturbation method for computing field distortions due to conductive regions with h-conform magnetodynamic finite element formulations," IEEE Trans. Magn., vol. 43, no. 4, pp. 1293-1296, 2007.

[7] Z.Ren, "Degenerated Whiney prism elements-general nodal and edge shell elements for field computation in thin structures" IEEE Trans. Magn., Vol. 34, No. 05, pp.2547-2550, 1998.

[8] C. Geuzaine, B. Meys, F. Henrotte, P. Dular and W. Legros, "A Galerkin projection method for mixed finite elements," IEEE Trans. Magn., Vol. 35, No. 3, pp. 1438-1441, 1999.

[9] Tsuboi, H., Asahara, T., Kobaysashi, F. and Misaki, T. (1997), "Eddy current analysis on thin conducting plate by an integral equation method using edge elements," IEEE Trans. Magn., Vol. 33, No. 2, pp. 1346-9.

[10] C. Guerin, G. Tanneau, G. Meunier, X. Brunotte and J.B. Albertini, "Three dimensional magnetostaic finite elements for gaps and iron shells using magnetic scalar potentials," IEEE Trans. Magn., Vol. 30, No. 5, pp.2888, 1994.

[11] X. Brunotte and G. Meunier, "Line element for efficent comuptation of the magnetic field created by thin iron plates," IEEE Trans. Magn., vol. 26, no. 3, pp. 2196-2198, 1990.